Bažant, Z.P. (1983). "Fracture in concrete and reinforced concrete," Preprints, IUTAM Prager Symposium on *Mechanics of Geomaterials: Rocks, Concretes, Soil*, ed. by Z.P. Bažant, Northwestern University, Evanston, 281–316.

PROGRAM

'ILLIAM PRAGER SYMPOSIUM

on

MECHANICS OF GEOMATERIALS: ROCKS, CONCRETES, SOILS

under the auspices of

International Union of Theoretical and Applied Mechanics

IUTAM

Department of Civil Engineering
and
Center for Concrete and Geomaterials

The Technological Institute

Northwestern University

Evanston, Illinois 60201 USA

September 11 – 15, 1983

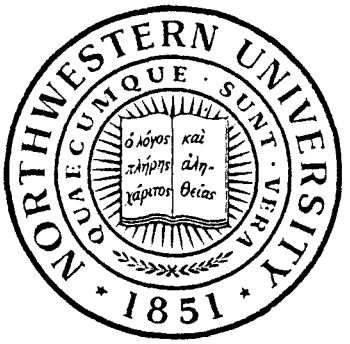

FRACTURE IN CONCRETE AND REINFORCED CONCRETE

Zdeněk P. Bažant
Professor of Civil Engineering
The Technological Institute
Northwestern University
Evanston, Illinois 60201, U.S.A.

Introduction

Although cracking represents a salient feature of the behavior of concrete structures, not only under ultimate loads but also at service states, fracture mechanics has not been used in practical analysis of structures. Structural engineers had a good reason; the linear fracture mechanics was found to be inapplicable to typical concrete structures, and the premises of ductile fracture mechanics did not match material behavior. However, in various recent investigations, particularly those at the Technical University of Lund, Northwestern University, and Politecnico di Milano, it has been shown that fracture mechanics can be applied to concrete structures provided that one takes into account the effect of a large micro-cracking zone or fracture process zone that always exists at the fracture front. The objective of the present paper is to review the results of the investigations at Northwestern University, many of them carried out under a cooperative agreement with Politecnico di Milano. It is not possible to include a comprehensive review of all the work on fracture of concrete; other work may be consulted for that [1-6].

Blunt Crack Band Model

The simplest way to model cracking in a finite element program is to assume that the cracks are continuously distributed over the area of the

finite element and manifest themselves by a reduction of the elastic modulus in the direction normal to the cracks. Complete cracking corresponds to a reduction of the elastic modulus to zero. In this description, introduced by Rashid [7], the crack band front cannot be narrower than the width of the frontal finite element. At the same time, the width of the crack band front cannot be wider than a single element. Of course, one could enforce the crack front to be of a multiple-element width, however, that would not be justified mechanically since one finds that localization of strain into a single-element width generally leads to a release of elastic energy. There is a further reason why a multiple-element width at the crack front is not a correct model; if we make the loading step sufficiently small, then only one element cracks during the loading step, and this relieves the stresses in the finite element that is on the side of the element that has just cracked, thus preventing an increase of the crack front width, except if a uniform strain distribution is enforced by heavy reinforcement. Even if two finite elements at the crack front had exactly the same stress values, it would be unrealistic to assume that they both crack simultaneously since the statistical scatter of material properties will always cause one of these elements to crack before the other does. Thus, one may adopt the blunt crack band model with a single-element wide front as a realistic and numerically very convenient model for cracking in concrete [10-16]. A similar approach can be applied to rock [10, 17].

Regardless of whether the zone of microcracking at the fracture front in concrete is very wide or not, two elementary justifications may be offered for the blunt crack band model. One of them is the heterogeneity of the material. We treat the material as a smoothed, homogeneous continuum in

the macroscopic sense. In this treatment, the macroscopic stresses and strains represent the averages of the actual (microscopic) stresses and strains over a certain so-called representative volume of the material which must be at least several times the maximum aggregate size in cross section.* Obviously, the rapid and scattered variation of stresses and strains over smaller distances cannot be described by a continuum approach. Therefore, using finite elements of sizes less than several times the aggregate size would not allow any improvement in the description of the actual stress and strain fields within concrete. Even if one wishes to treat a continuous sharp crack in concrete, the blunt crack band model does not represent the reality any worse than a sharp inter-element crack model because the actual crack path is not straight but highly tortuous.

As another justification, of the blunt crack band model for describing sharp fractures in concrete, one may cite the recently documented fact that a sharp inter-element crack and a blunt crack band of single-element width yield approximately the same results for not too crude meshes (roughly when there are at least fifteen finite elements in a square mesh across the cross section). Both models give energy release rates that differ not more than a few percent from the exact elasticity solution. To illustrate it, Fig. 2 exhibits some of the numerical results from Ref. 12. In these calculations, the normal stress in the direction perpendicular to the cracks was assumed to drop suddenly to zero when the energy criterion for crack band propagation became satisfied. The finite element mesh in Fig. 2 covers a cut-out of an infinite elastic medium loaded at infinity by uniform normal stress $\bar{\sigma}$ perpendicular to a line crack of length 2a. The nodal loads applied at the mesh boundary are calculated as the resultants of the exact

*See Fig. 1

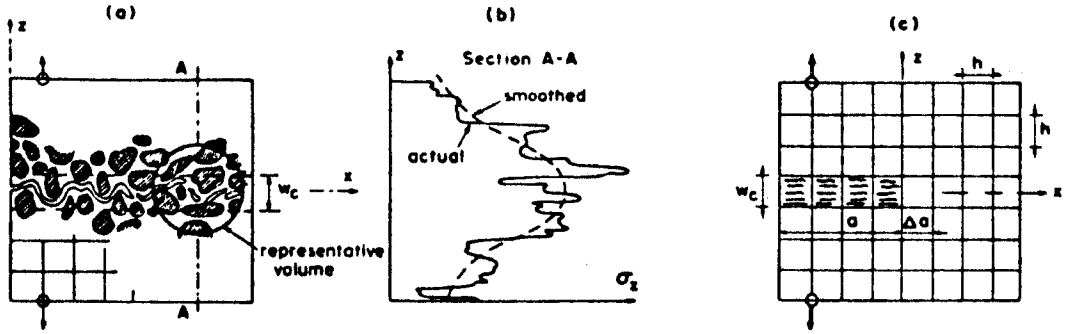

Fig. 1 - Heterogeneous Microstructure, Random Scatter of Stresses and Strains; Plots of Bažant and Cedolin (1979).

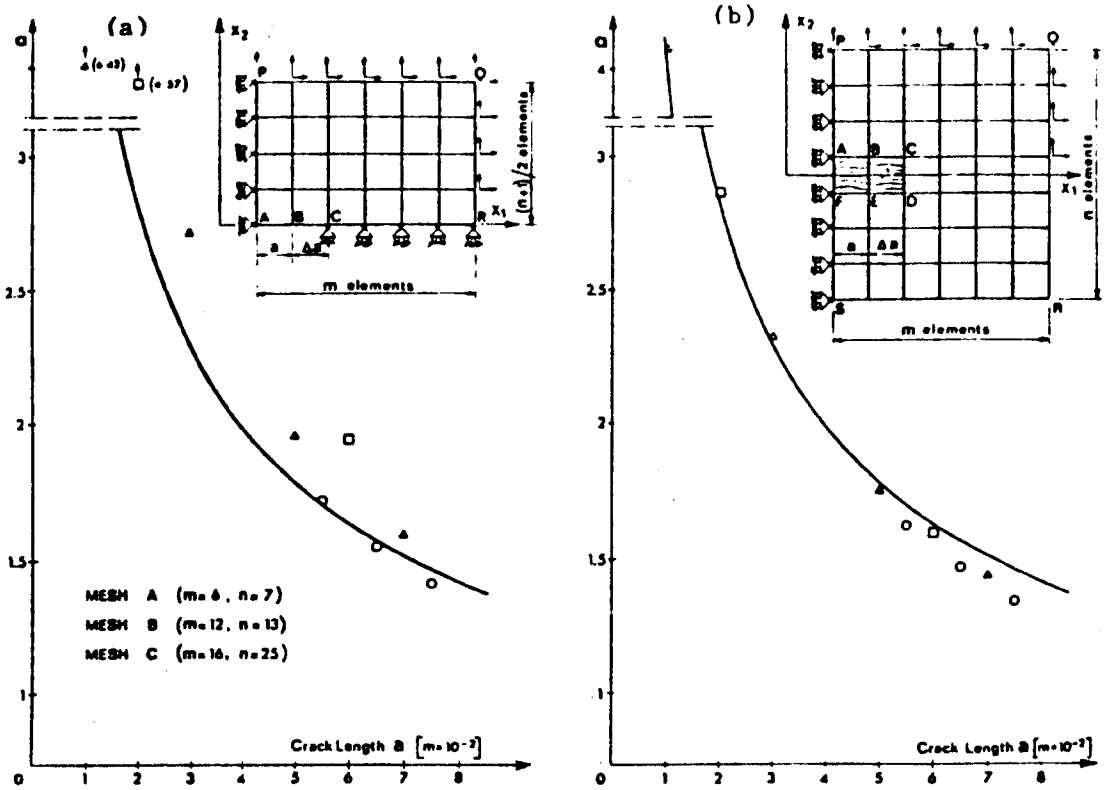

Fig. 2 - Finite Element Results of Bažant and Cedolin (1977) (for Sudden Stress Drop) Showing Equivalence of Blunt Crack Band and Sharp Crack Modeling.

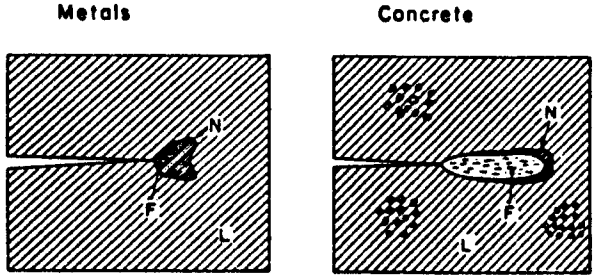

Fig. 3 - Nonlinear Zone and Fractur Process Zone for Various Materials.

stresses in the infinite medium, based on Westergaard's exact solution which is shown as a solid curve. The data points in Fig. 2 show numerical results for the square mesh shown (mesh A), as well as for finer meshes B and C (not shown) for which the element size was 1/2 and 3/8 of the element size shown, respectively. A similar equivalence of results for the sharp inter-element crack and the blunt crack band can be demonstrated when the stress is considered to drop gradually rather than suddenly to zero [11].

Aside from the foregoing justifications, the blunt crack band model appears to be more convenient for finite element analysis. When a sharp inter-element crack extends through a certain node, the node must be split into two nodes. This increases the total number of nodes and changes the topological connectivity of the mesh. Unless the nodes are renumbered, the band structure of the structural stiffness matrix is lost. Moreover, if the direction in which an inter-element crack should extend is not known in advance, one needs to make trial calculations for various possible locations of the node ahead of the crack front through which the crack should pass, in order to determine the correct direction of crack propagation. On the other hand, in the blunt crack band model, a fracture propagating in any direction through the mesh can be modeled as a zig-zag crack band with any direction of the cracks relative to mesh lines. All that needs to be done to model an oblique crack direction is to reduce the elastic stiffness in the direction normal to the cracks.

Recently, various attempts to observe the distribution of microcracks ahead of the fracture front in concrete have been made [18-20]. From strain measurements by Moiré interferometry [19, 20], it appears that the width of the

microcrack zone at the fracture front is about one aggregate size. Within this width, there is a crack concentration. However, the line along which the most dense microcracks are scattered is not straight but rather tortuous (Fig. 1), which would not be modeled by a straight inter-element crack any better than by a crack band. Correlation of the crack band model to such microscopic observation is, of course, difficult since the microcrack density varies while in the crack band it is assumed to be uniform. The question then is at which microcrack size to draw the distinction. Thus, the width of the microscopally observed crack band front depends on the definition of the width of the microcracks that are counted within the crack band.

One significant difference from ductile fracture of metals consists in the size of the fracture process zone, defined as the zone in which the material undergoes strain-softening, i.e., the maximum principal stress decreases at increasing strain. This zone is large for concrete but relatively small for metals, even in the case of ductile fracture. In the latter case, there is a large yielding zone, but the material does not soften in this zone (Fig. 3).

The stress-strain relation with strain-softening for the fracture process zone may be replaced by a strain-displacement relation if the displacement represents the integrated value of the strains across the width of the crack front. In this sense, the present blunt crack band model is equivalent to the previous line crack models with softening stress-displacement relations, introduced by Knauss, Wnuk, Kfouri, Miller, Rice and others [21-27]. For concrete this approach was pioneered by Hillerborg, Modéer and Petersson [27, 28] in their model of a fictitious sharp inter-element crack.

Let us now outline one possible form of the softening stress-strain relation for the fracture process zone. Let the virgin crack-free materia. be described by the elastic stress-strain relation

$$\underset{\sim}{\varepsilon} = \underset{\sim}{C}\,\underset{\sim}{\sigma} \tag{1}$$

Here, $\underset{\sim}{\sigma}$, $\underset{\sim}{\varepsilon}$ are the column matrices of the cartesian normal components of strain and stress, in cartesian coordinates $x_1 = x$, $x_2 = y$, and $x_3 = z$. $\underset{\sim}{C}$ is a 3 x 3 square compliance elastic matrix of the virgin material, with components C_{11}, C_{12},...C_{33}. For the sake of simplicity, we may now assume that all microcracks spread over the finite element are normal to axis z. Appearance of such cracks has no effect on the lateral strains ε_x and ε_y, and the only effect is an increase in the averaged normal strain ε_z in the direction perpendicular to the cracks. This may be described by cracking parameter μ introduced only in one diagonal form of the compliance matrix [10, 11], i.e.,

$$\underset{\sim}{C}(\mu) = \begin{bmatrix} C_{11} & C_{12} & C_{13} \\ & C_{22} & C_{23} \\ & & C_{33}\mu^{-1} \end{bmatrix} \tag{2}$$

The cracking parameter μ is 1 for the initial crack-free state, and approaches 0 for the final fully cracked state. It has been shown [11], that the limit of the inverse of the compliance matrix $C(\mu)$ as $\mu \to 0$ is, exactly, the well-known stiffness matrix for a fully cracked elastic material, D^{fr}. This matrix is identical to the elastic stiffness matrix for the plane state of stress, which exists in the material between the cracks.

The cracking parameter may be calibrated so as to yield the desired tensile stress-strain relation with strain-softening, $\sigma_z = EF(\varepsilon_z)$, in which

$E = 1/C_{33}$ = Young's modulus. Then one has $\mu = F(\varepsilon_z)/\varepsilon_z$. Function $F(\varepsilon_z)$ may be given as a bilinear stress-strain diagram (Fig. 4), characterized by tensile strength f_t', softening modulus E_t (negative), and limit strain ε_0 for which full cracks are formed. For computer analysis, the foregoing stress-strain relation is differentiated to obtain an incremental form to be used in a program with step-by-step loading.

The strength limit f_t', needs adjustment to take into account the effect of multiaxial stress state. In particular, the tensile strength limit is decreased due to normal compressive stresses σ_x and σ_y parallel to the crack plane. Correction may be done according to the well-known biaxial failure envelope for concrete [11].

The use of cracking parameters μ resembles the so-called continuous damage mechanics, in which damage is characterized by parameter ω which corresponds to $1 - \mu$. There is, however, a fundamental difference in that the damage due to microcracking is considered to be inseparable from a zone of a certain charasteristic width that is a material property, as we will explain later.

The energy consumed by crack formation per unit area of the crack plane, i.e.,

$$G_f = W_f w_c, \qquad W_f = \int_0^{\varepsilon_0} \sigma_z \, d\varepsilon_z \tag{3}$$

represents the fracture energy; w_c = width of the crack band front (fracture process zone), and W_f = work of maximum principal tensile stress per unit volume = area under the uniaxial tensile stress-strain curve (Fig. 4).

The magnitude of w_c is obviously an important factor. If the stress-strain relation, including its strain-softening range, is considered to be

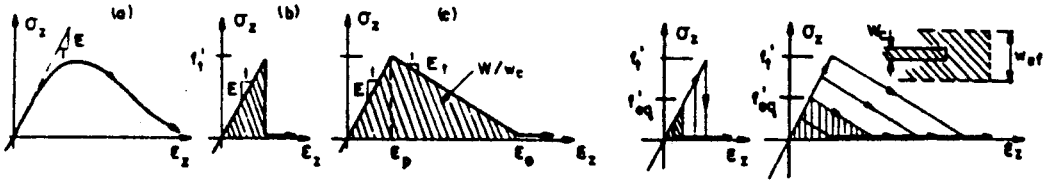

Fig. 4 - Tensile Stress-Strain Diagrams Assumed for Fracture Analysis.

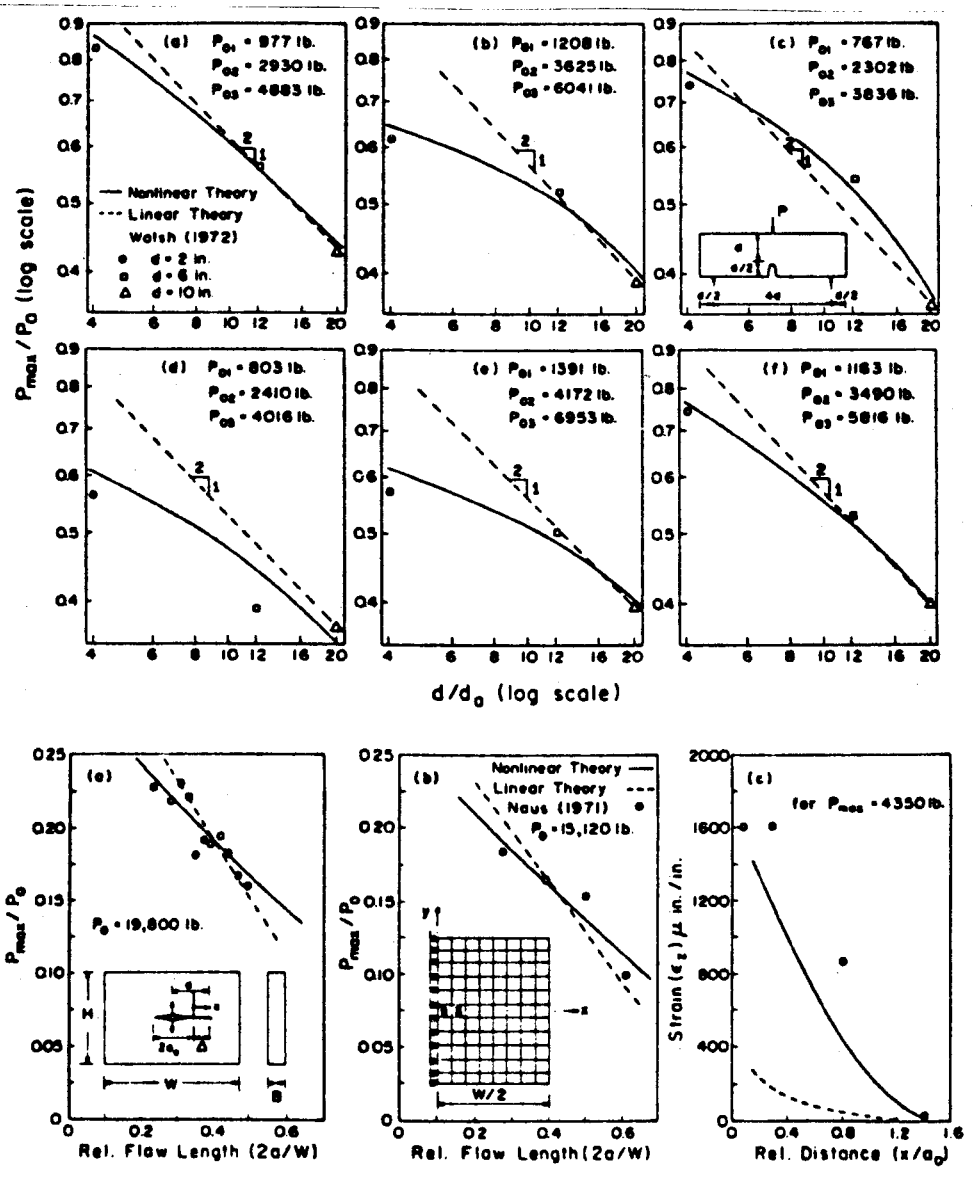

Fig. 5 - Results of Crack Band Analysis Compared With Maximum Load Test Data from the Literature (after Bažant and Oh, 1983).

a material property, which seems logical, then the larger w_c is the larger is the fracture energy G_f. However, it has been previously demonstrated [12, 13] that finite element calculations yield results independent of the choice of the element size (except for a negligible numerical error), only if the fracture energy G_f is considered as a material constant. Eq. 3 then indicates that the width w_c of the crack band front must also be a material constant, to be determined by tests. Indeed, if the value of w_c is changed without adjusting the strength limit f_t' or the strain-softening modulus E_t, the predicted values of loads needed for further crack propagation may change drastically [12, 13]. For the bilinear tensile stress-strain relation (Fig. 4), we have $W_f = \frac{1}{2}(C_{33} - C_{33}^t)f_t'^2 w_c = \frac{1}{2} f_t' \varepsilon_0$ or

$$w_c = \frac{2G_f}{f_t'^2} \frac{1}{C_{33} - C_{33}^t} \tag{4}$$

in which $C_{33}^t = 1/E_t$ (negative). Thus, the width of the crack band front may be determined by measuring the tensile strength, the fracture energy, and the softening modulus E_t. Note that Eq. 4 is similar to the well-known Irwin's expression for the size of the yielding zone. It should be also noted that determination of w_c from mechanical measurements depends on the knowledge of the strain-softening slope E_t. If this slope is changed, a different value of w_c is obtained, and fracture test data may still be fitted equally well, within a certain range of w_c. In fitting test data for concrete fracture from the literature, it has been noted that good fits could be obtained for w_c ranging from $2d_a$ ti $4d_a$ where d_a is the maximum aggregate size. The front width

$$w_c = 3d_a \tag{5}$$

was nearly optimum, and at the same time was consistent with the softening modulus E_t as observed in the direct tension tests of Evans and Marathe [32].*

Most of the important test data from the literature [33-49], have been fitted with good success using the present nonlinear fracture model [11]. Some of the fits obtained in Ref. 11 by finite element analysis using square meshes are shown in Figs. 5 and 6, in which P_{max}, representing the maximum measured load, is plotted as a function of either the crack length (flaw depth) or the specimen size. The optimum fits obtainable with linear fracture mechanics are shown for comparison in these figures as the dashed lines. The loading point was displaced in small steps in computations, and the reaction, representing load P, was evaluated at each loading step by finite elements. The same bilinear stress-strain relation was assumed to hold for all elements.

Note that the crack band approach to fracture models well not only the results for notched fracture specimens, but also the results for unnotched beams, in which the nominal bending stress at failure decreases as the beam depth increases (Fig. 5). This phenomenon is due to the fact that the large fracture process zone (strain-softening zone) cannot be fully accommodated in a small beam. The same phenomenon was previously modeled as a statistical size effect; however, explanation in terms of fracture mechanics, previously proposed by Hillerborg, appears to be the correct one.

Deviations from linear fracture mechanics have been also described for metals by the so-called R-curves (resistance curves), which represent the variation of apparent fracture energy as a function of the crack extension from a notch. Based on an original proposal by Krafft et al. [50], the R-curve may be considered for most situations as a fixed material property,

---

*Strain-softening in direct tensile tests of concrete has been also documented in Refs. 51-53 and 49.

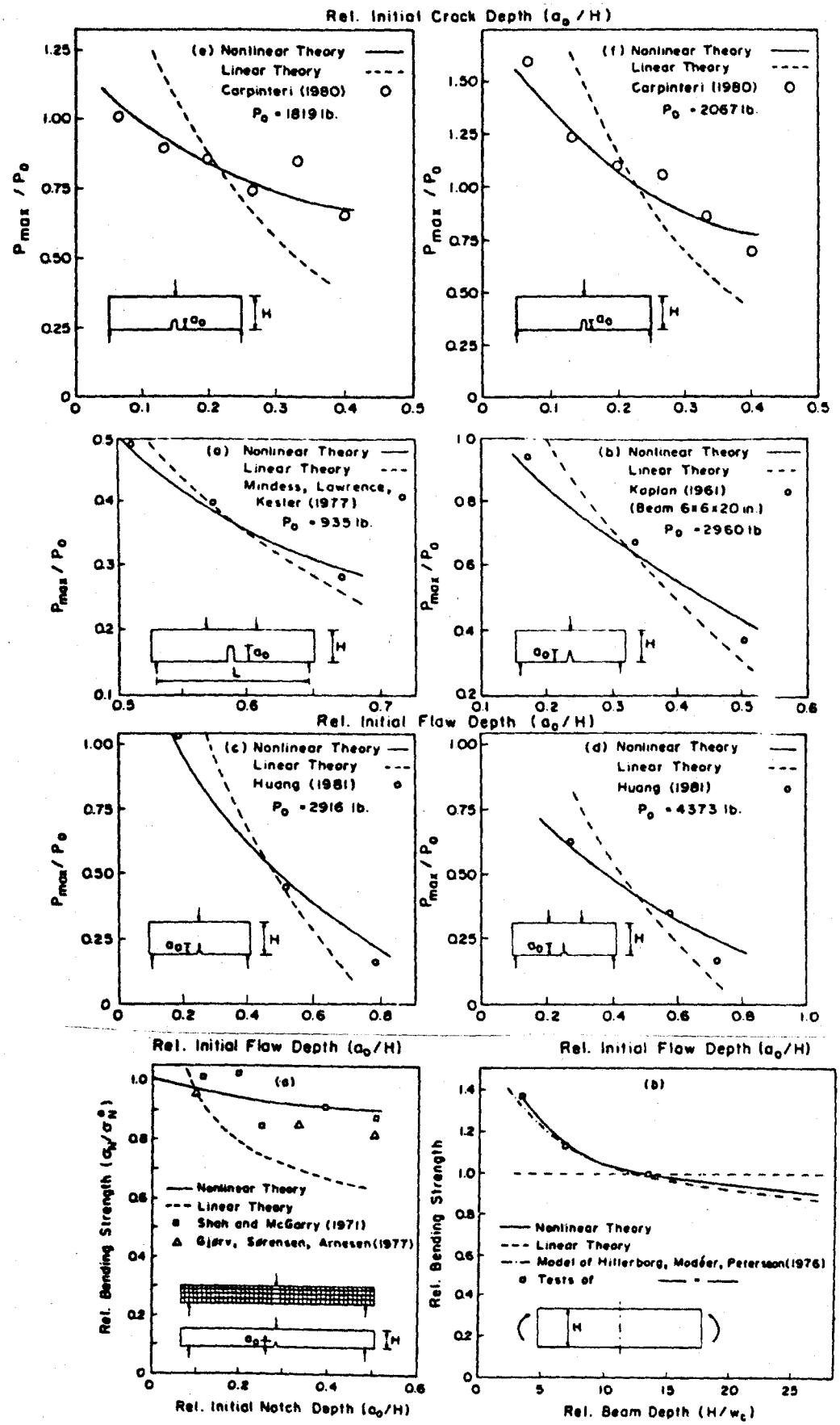

Fig. 6 - Crack Band Calculation Results Compared With Further Maximum Load Test Data From the Literature (after Bažant and Oh, 1983).

although in reality it may be such only asymptotically, for infinitely small crack extensions from a notch (for longer extensions, the R-curve should, in theory, also depend on the boundary geometry, location of the loads, crack path, etc.). It is noteworthy that the present theory achieves a good fit of test data without introducing any variation of fracture energy G_f, i.e., G_f is a constant. In fact, the present theory allows calculating the R-curves. For this purpose one needs to evaluate the work of the nodal forces acting at the crack front element during a small crack band extension. In this manner the R-curves have been calculated, using the same fracture parameters as in the previous fitting of maximum load data. These calculations have led to good fits of R-curve data reported in the literature [11]; see Fig. 7, using test data from Refs. 33, 36, 45, and 48. For the details of analysis, see Ref.11. (It is worth noting that the present theory has been also used with equal success to fit the test data for various rocks [10, 17].)

Statistical analysis of the test data available in the literature revealed that the crack band theory allows a great reduction of the coefficient of variation ω_0 of the deviations of test data from the theory. In the case of maximum load data, $\omega_0 = 0.666$, while for the best fits with linear elastic fracture mechanics, $\omega_0 = 0.267$. For the strength criterion, $\omega_0 = 0.650$. In the case of R-curves, the present crack band theory yields standard deviation for the deviations of test data from the theory as $s = 0.083$, while linear fracture mechanics with constant fracture energy yields $s = 0.317$; see Ref. 11. These are significant improvements in the error statistics, and the present crack band theory is seen to be sufficient for practical purposes. The analysis of test data from the literature allowed it also to set up an approximate

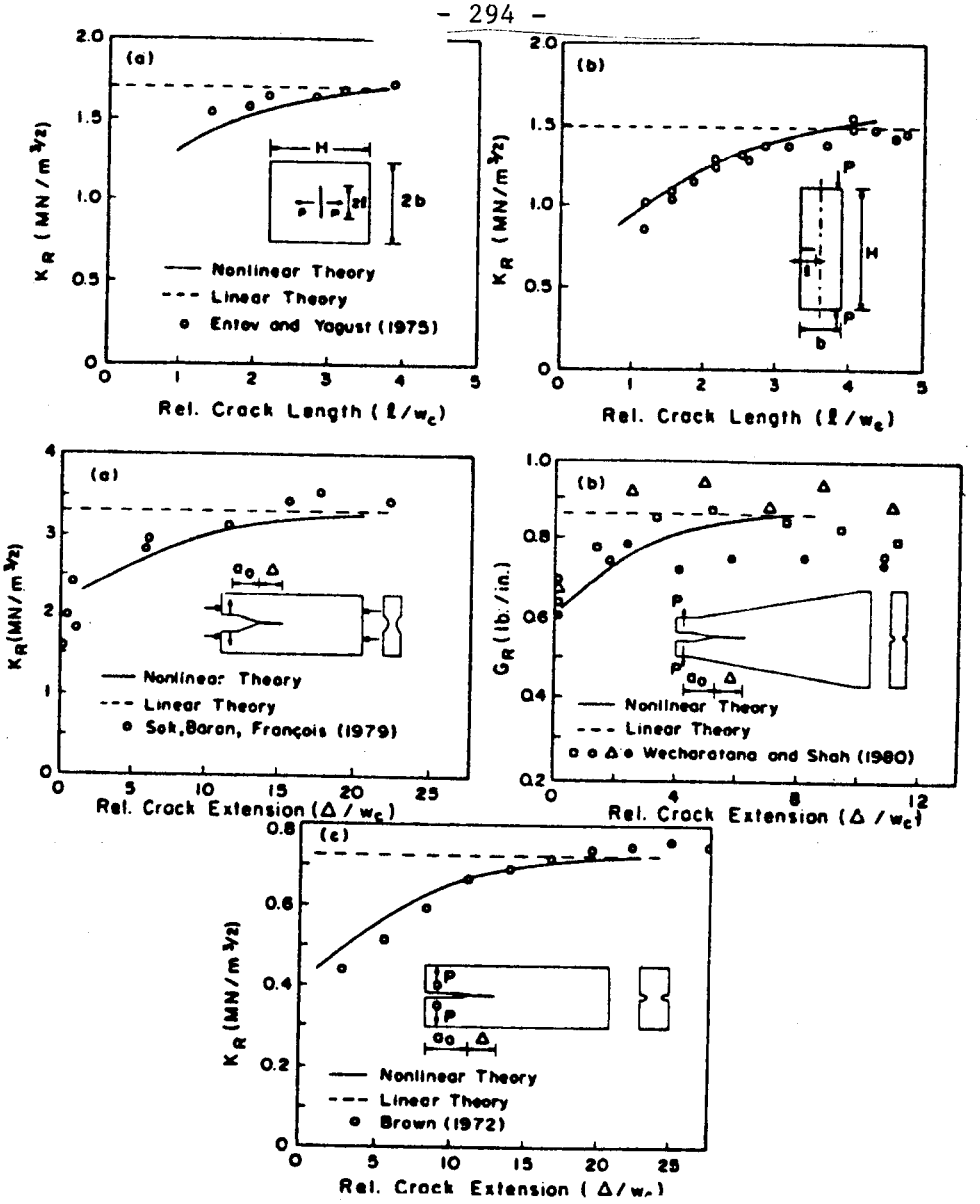

Fig. 7 - Crack Band Calculation Results Compared with Measured R-Curves from the Literature (after Bažant and Oh, 1983).

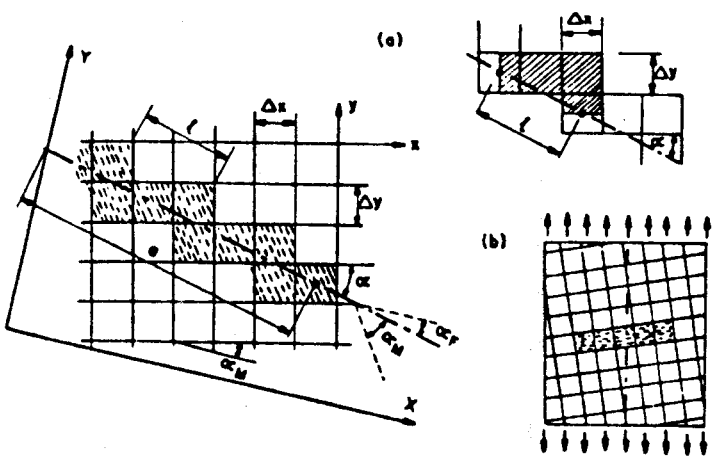

Fig. 8 - Zig-Zag Crack Band Propagation through a Square Mesh.

empirical formula for the prediction of fracture energy on the basis of tensile strength f'_t, maximum aggregate size d_a, and Young's modulus E;

$$\tilde{G}_f \simeq 0.0214(f'_t + 127)f'^2_t\, d_a/E \tag{6}$$

in which f'_t must be in psi (psi = 6895 Pa), and $\tilde{G}_f$ is in lb./in. Exploiting the relation $G_f \simeq 3d_a\, f'^2_t(E^{-1} - E_t^{-1})/2$, one can further obtain a prediction formula for the softening modulus

$$E_t \simeq \frac{-69.9E}{f'_t + 56.7} \tag{7}$$

Application in Finite Element Programs

Finite elements of size $h = w_c = 3d_a$ may be too small for many practical applications. However, we cannot simply increase the element size because according to Eq.3 the energy consumed by fracture would increase proportionally with h, other parameters remaining unchanged. Obviously, in order to maintain the same energy consumption by fracture, the area under the tensile stress-strain diagram must be changed in inverse proportion to the element width h. This may be done most conveniently by adjusting the strength limit from the actual strength f'_t to an equivalent tensile strength f'_{eq}. If we use the bilinear stress-strain diagram and keep the softening modulus E_t constant, we obtain the following expression for the equivalent strength in a square mesh in which the fracture propagates parallel to the mesh line;

$$f'_{eq} = c_f\left(1 + \frac{E}{-E_t}\right)^{-\frac{1}{2}} \left(\frac{2G_f E'}{w_h\, r_f}\right)^{\frac{1}{2}} \tag{8}$$

in which c_f is a calibration factor close to 1, depending on the type of finite element, and r_f is a correction for the compressive normal stress parallel to the crack plane ($r_f = 1 - \nu'\, \sigma_3/\sigma_1$).* We see that the tensile strength limit must be reduced in inverse proportion to the square root of element size.

---

*Here $\nu' = \nu/(1 - \nu)$, ν = Poisson ratio.

If the tensile strength limit is not changed when the element size changes, fracture analysis is unobjective in that the results may strongly depend on the analyst's choice of the element size. A glaring example of this was presented in Ref. 15 in which a rectangular panel, either plane or reinforced, was analyzed for propagation of a symmetric central crack band. It was demonstrated that by changing the element size four times, the calculated value of the load needed for further crack band propagation changed this by a factor of 2 (i.e., by 100%). (If the element size is much larger than w_c, the value of equivalent strength f'_{eq} is very small and may be neglected. Then one obtains the no-tension material pioneered some twenty years ago by Zienkiewicz et al.)

Keeping the strength limit the same regardless of the element size does not necessarily lead to wrong results. In fact, in many situations finite element analyses with a constant tensile strength yielded good results, in agreement with tests. The reason why this happens is that many structures are fracture-insensitive, i.e., their failure depends primarily on other phenomena such as plastic yielding of steel rather than on cracking of concrete. The flexural failure of reinforced beams is a good example. To decide whether the problem is fracture-insensitive, the analyst needs to run the finite element calculations twice: once with the actual tensile strength f'_t, and once with a zero tensile strength. If the results do not differ significantly, one may forget about adjusting the tensile strength limit.

For structures much larger than the aggregate size, the size of the fracture process zone may become negligible compared to the cross section dimensions (this is true, e.g., for gravity dams). If the finite elements are not very small, a small fracture process zone can be obtained by considering

a vertical stress drop instead of gradual strain-softening. A small fracture process zone is a prerequisite for the validity of linear elastic fracture mechanics, and indeed it is found [10, 11] that the use of a sudden stress drop after the tensile strength limit has been reached leads to results that are very close to the exact solutions of linear elastic fracture mechanics. The results with the present crack band model are just as close to the exact solution as those obtained with the sharp interelement crack model [10].

When a vertical stress drop is assumed, the energy criterion of fracture mechanics can be more closely approximated by a direct calculation of the energy release due to crack band extension, rather than the use of a specified tensile stress-strain diagram with equivalent strength. A formula for the change in potential energy due to crack band extension was given in Refs. 10 and 11. In this formula, one calculates the work of the nodal forces acting upon the frontal finite element during the fracture formation. One must also consider the differences between the initial and final strain energy within the cracked frontal finite element, as well as the work of distributed forces transmitted by reinforcement on concrete.

Instead of directly calculating the work of nodal forces on the frontal finite element, one may also obtain the exact energy release through the use of the J-integral. This method of analysis was developed by Pan and coworkers [54].

An important advantage of the blunt crack band model is that the direction of mesh lines need not be changed if the fracture runs in a skew direction. The crack band propagation criterion then requires some adjustment in order to give results that do not depend on mesh inclination.

We consider a rectangular mesh of mesh sizes Δx and Δy (Fig. 8). An inclined crack band is represented as a zig-zag crack band of overall orientation angle α_F. Let α_M be the orientation angle of the mesh lines x, and α_C be the direction of the cracks within the finite element (Fig. 9). We seek the effective width w_{ef} of a smooth crack band that is equivalent to the zig-zag band. Consider one cycle, of length ℓ, on the line connecting the centroids of the elements in the zig-zag band. The number of elements per cycle ℓ in the x-direction is $N_x = \ell \cos\alpha/\Delta x$, and the number of those in the y-direction is $N_y = \ell \sin\alpha/\Delta y$ in which $\alpha = |\alpha_F - \alpha_M|$ provided that $0 \leq \alpha \leq 90^o$. The area of the zig-zag band per cycle ℓ is $(N_x \Delta y)\, \Delta x + (N_y \Delta_x)\, \Delta y$. This area must equal the area $\ell\, w_{ef}$ of the equivalent smooth crack band, in order to assure the same energy content at the same stresses. This condition yields the effective width

$$w_{ef} = \Delta x \sin\alpha + \Delta y \cos\alpha \qquad (0 \leq \alpha \leq 90^o) \tag{9}$$

A somewhat different equation, giving similar results for $\alpha \leq 45^o$ has been used in previous work [13-15].

A different adjustment is needed when one considers a sudden stress drop and determines crack propagation directly from the energy change ΔU caused by extending the crack band into the next element. The propagation condition then is $\Delta U/\Delta a = -G_f$ where Δa is the length of extension of the crack band, which is equal to the mesh size h if the crack band propagates parallel to the mesh line [12, 13, 6]. In the case of a zig-zag band, Δa must be replaced by an effective crack band extension Δa_{ef} in the direction of the equivalent smooth crack band. We may assume Δa_{ef} to be the same for each crack band advance within the cycle ℓ in Fig. 8, whether this advance is in the x- or y-direction. Then $\Delta a_{ef} = \ell/N$ where $N = N_x + N_y$ = number of

elements per cycle ℓ. This condition yields

$$\Delta a_{ef} = \left(\frac{\cos \alpha}{\Delta x} + \frac{\sin \alpha}{\Delta y}\right)^{-1} \qquad (0 < \alpha < 90^{o}) \tag{10}$$

It has been demonstrated that the calculation results are objective not only with regard to the choice of element size but also with regard to the choice of mesh inclination relative to the fracture direction. Meshes of various inclination have been used to calculate the load— crack-length diagram for the rectangular panel considered before; they have been found to yield essentially the same results, except that the scatter (numerical errors) are somewhat larger for the zig-zag crack bands than for a smooth band; see Ref. 15.

It is one problem when the fracture direction is known and the zig-zag crack band is placed so as to conform to the average fracture direction, and another problem when the fracture direction is unknown in advance and a choice of the next element to crack must be made. The latter problem is obviously more difficult. It has been found that any finite element mesh, including a square mesh, is not entirely free of a directional bias. This bias is the strongest when the angle of fracture direction with the mesh line is small. For example, if a square mesh in the center-cracked rectangular panel is only moderately slanted (Fig. 8b), then the equivalent strength criterion with the effective width given by Eq. 8 indicates the crack band to extend straight along the mesh line, i.e., in the inclined direction, while correctly there should be side jumps so that the zig-zag band would, on the averate, conform to a horizontal direction. It appears rather difficult to avoid this type of bias. Various methods to avoid it are being studied [55-58]. Some search routines to determine which element

is the next to crack (the element straight ahead or the element on the left or on the right) are being investigated.

When concrete is reinforced, attention must also be paid to the question of bond slip of reinforcing bars embedded in concrete. It has been shown [13], that neglect of the bond slip is impossible, leading to unobjective results strongly dependent on the mesh size and converging to a physically incorrect solution. If no slip is considered to occur at the nodes between the bars and concrete, and if the element size is varied, then the stiffness of the connection between the opposite sides of a fracture changes with the mesh size and would approach infinity for a vanishing mesh size, thus preventing any crack propagation at all. In reality, due to a limit on the bond stress that can be transmitted on the surface of a steel bar, there is a certain bond slip length L_s on each side of a crack band. This length depends on the bar cross section A_b, ultimate bond force U_b', ratio n' of the elastic moduli of steel and concrete, stress σ_s in the bars at the point of crack band crossing, and the reinforcement ratio p (the bars are assumed to be spaced regularly and densely). The following expression was derived [13],

$$L_s = \frac{A_s}{U_b'} (\sigma_s - \sigma_s') \simeq \frac{A_b}{U_b'} \frac{1 - p}{1 - p + n'p} \sigma_s \tag{11}$$

For convenience of programming it is further possible to replace this actual bond slip length with an equivalent free bond-slip length L_s^* which coincides with a distance between certain two nodes within the mesh, and which permits neglecting the bond shear stresses that are difficult to model in a finite element code. The cross section area A_b must also be adjusted to a value A_b^*. The values of L_s^* and A_b^* are then determined from the condition that the extension of the steel bar over the length L_s, with bond shear stresses present, would be the same as the extension of a bar of cross section area A_b^* and length L_s^* with zero bond stresses; see Ref. 13.

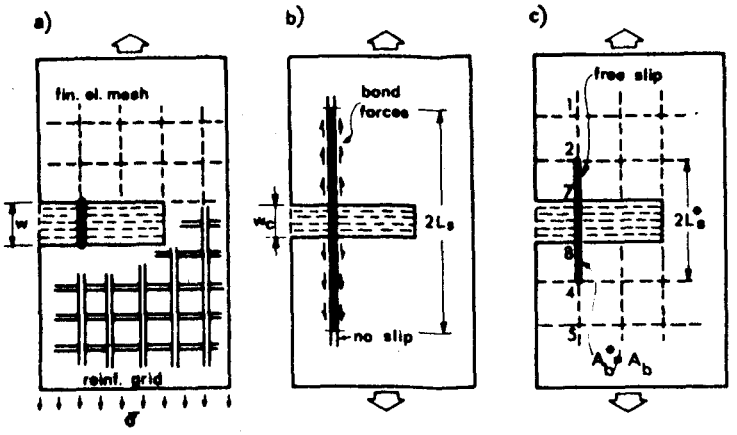

Fig. 9 - Illustrations of Bond Slip and Equivalent Free Bond Slip Length (after Bažant and Cedolin, 1980).

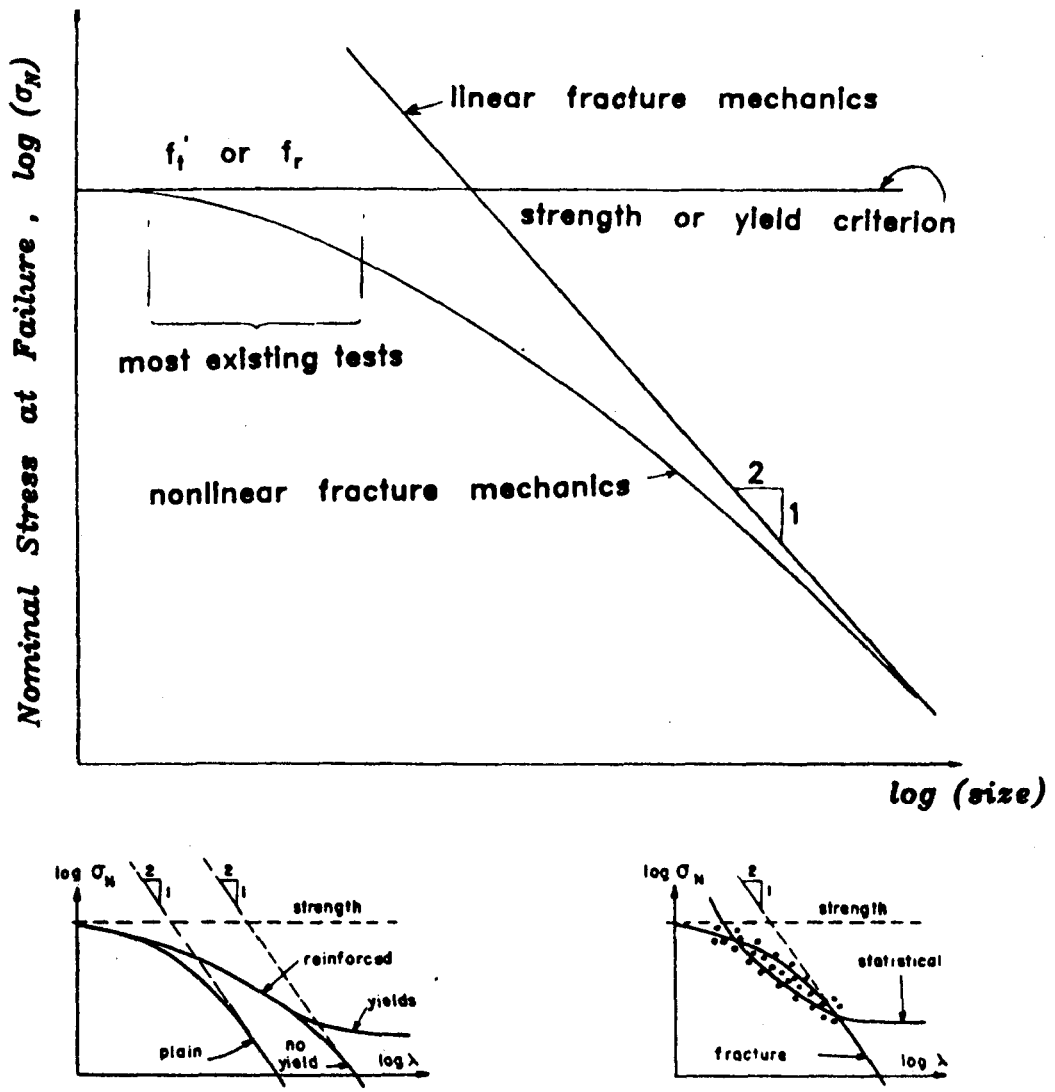

Fig. 10 - Various Theories for Structural Size Effect.

When reinforcement is used, the expression for the equivalent strength must also be adjusted. The following formula has been derived from energy release considerations [6, 15];

$$f'_{eq} = c_f\left(\frac{2G_f E_c}{w_{ef} r_f}\right)^{\frac{1}{2}} \left(1 + c_p \; n' \frac{p}{L_s^*} \cos\alpha_s\right) \qquad (12)$$

in which α_s = angle of the reinforcing bars with the normal to the crack band, and c_p is an empirical coefficient to be found by numerical calibration, i.e., comparisons of results for different mesh sizes [15].

It might be more realistic to treat reinforcement and bond slip by introducing two overlaid continuua, one representing the plane concrete, and one representing the reinforcement mesh. These continuua would be allowed to displace relative to each other and would transmit distributed volume forces from one to another, depending on the relative slip. This approach would be, however, much more complicated.

Structural Size Effect

The dispersed and progressive nature of cracking at the fracture front may be taken into account by introducing the following hypothesis [59]: The total potential energy release W caused by fracture in a given structure depends on both:

1) The length a of the fracture, and

2) The area of the cracked zone, a n d_a

in which n is a material constant characterizing the width of the cracking zone at the fracture front [11], n ≃ 3. The dependence of W upon crack length a describes that part of energy release that flows into the fracture front from the surrounding uncracked regions of the structure.

Parameters a and a_n d_a are not nondimensional. They are permitted to appear only in a nondimensional form, which is given by the following nondimensional parameters

$$\alpha_1 = \frac{a}{d}, \qquad \alpha_2 = \frac{\text{and}_a}{d^2} \tag{13}$$

They represent the nondimensional fracture length and the nondimensional area of the crack zone. Furthermore, W must be proportional to volume d^2b of the structure, b denoting the thickness, and to the characteristic energy density $\sigma_N^2/2\ E_c$ in which $\sigma_N = P/bd$ = nominal stress at failure, P = given applied load, and d = characteristic dimension of the structure. Consequently, we must have

$$W = \frac{1}{2E_c}\left(\frac{P}{bd}\right)^2 bd^2\ f(\alpha_1, \alpha_2, \xi_i) \tag{14}$$

in which f is a certain continuous and continuously differentiable positive function, and ξ_i represent ratios of the structure dimensions characterizing the shape of the structure.

To illustrate the structural size effect, we now consider structures of different sizes but geometrically similar shape, including the same ratio of fracture length to the characteristic dimension of the structure, and the same reinforcement ratio. Under this assumption, the shape parameters ξ_i are constant. Using the energy criterion for crack band propagation, $\partial W/\partial a = G_f\ b$, in which G_f is the fracture energy, we obtain (for constant ξ_i) $\partial f/\partial a = f_1(\partial\alpha_1/\partial a) + f_2\ (\partial\alpha_2/\partial a)$ where we introduce the notations $f_1 = \partial f/\partial\alpha_1$, $f_2 = \partial f/\partial\alpha_2$. Substitution of Eq. 12 into Eq. 13 then yields

$$\left(\frac{f_1}{d} + \frac{f_2\, n d_a}{d^2} \right) \frac{P^2}{2bE_c} = G_f\, b \tag{15}$$

Here the fracture energy may be expressed as the area under the tensile stress-strain curve, i.e., $G_f = n\, d_a\, (1 - E_c/E_t)\, f_t'^2/2E_c$, in which E_c is the initial Young's elastic modulus of concrete, E_t is the mean strain-softening modulus, which is negative, and f_t' is the direct tensile strength of concrete. Substituting this expression for G_f together with the relation $P = \sigma_N\, bd$* into Eq. 14, we finally obtain

$$\sigma_N = Bf_t' \left(1 + \frac{d}{\lambda_0 d_a} \right)^{\frac{1}{2}} \tag{16}$$

in which $B = [(1 - E_c/E_t)/f_2]^{\frac{1}{2}}$, $\lambda_0 = mf_2/f_1$. B and λ_0 are constants when geometrically similar structures of different sizes are considered. In the plot of log σ_N versus $\log(d/d_a)$ where d/d_a is the relative structure size, Eq. 18 is represented by the curve shown in Fig. 10. If the structure is very small, then the second term in the parenthesis in Eq. 15 is negligible compared to 1, and $\sigma_N = B\, f_t'$ is the condition characterizing failure, representing the strength criterion which in Fig. 10 corresponds to a horizontal line. This special case is obtained if W depends only on the crack-zone area but not on the fracture length. If the structure is very large, then 1 is negligible compared to the second term in the parenthesis of Eq. 15. Then $\sigma_N = \text{const.}/\sqrt{d}$. This is the type of size effect known to apply for linear elastic fracture mechanics. Thus, linear elastic fracture mechanics must always apply for a sufficiently large concrete structure. It is interesting to note also that the preceding nondimensional analysis yields this limiting case when the starting hypothesis includes only dependence of W on the fracture length but not on the cracked zone area. In Fig. 15 the limiting case of linear fracture mechanics is represented by the straight line of downward slope - 1/2.

---

*Here σ_N = nominal stress at failure.

The size effect in concrete structures failing due to cracking of concrete represents, as we have shown, a gradual transition from the strength criterion to the energy criterion of linear fracture mechancis. Unfortunately, among the numerous test data on fracture of plain concrete as well as on brittle failures of concrete structures, as reported in the literature, only a very small fraction involves fractures of specimens of sufficiently different sizes to check our preceding conclusion. From fracture testing of plain concrete, the size effect may be checked from the test data of Walsh [47] (Fig. 6). A very good agreement with Eq. 15 is found from these data. As for brittle failure of concrete structures, a check can be made using certain data for the diagonal shear failures of concrete beams with longitudinal reinforcement but without stirrups. Results of such tests are shown in Fig. 11 for test data from Refs. 61-67. In spite of the large scatter, due to comparing test data from different laboratories for different concretes, the declining trend is obvious. A horizontal line, corresponding to the strength criterion (as well as to the present ACI or CEB-FIP codes), is contradicted by the test data. At the same time, however, one can clearly see a substantial deviation from the straight line representing linear elastic fracture mechanics. For more detail, see Ref. 60.

In the preceding analysis we have not paid any particular attention to reinforcement. If a densely and regularly distributed reinforcement is present, one finds that the size effect is again governed by Eq. 15, however, with different constants, provided that the reinforcement remains elastic. Compared to plain concrete, the asymptotic straight line for linear elastic fracture mechanics is pushed in the plot of Fig. 10 toward the right, i.e., there exists a greater range of sizes for which the strength criterion applies.

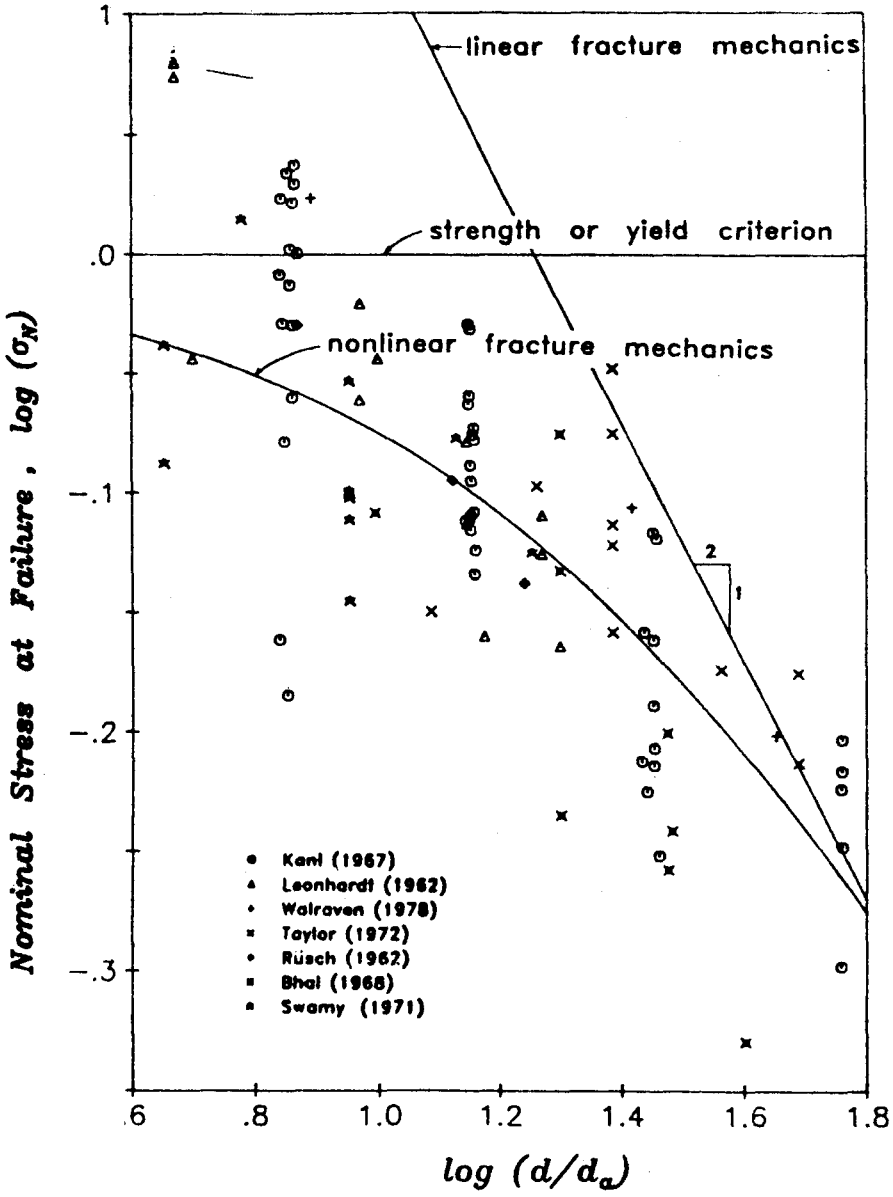

Fig. 11 - Test Data From Various Laboratories on Diagonal Shear Failure of Beams Reinforced Longitudinally but Without Stirrups (after Bažant and Kim, 1983).

Nevertheless, for sufficiently large structures, a transition to the size effect of linear fracture mechanics does occur. This conclusion, however, is true only if the reinforcement does not yield. If it does, then there is another transition in Fig. 10 to a horizontal asymptote (see Ref. 59).

The decrease of nominal stress at failure with the structure size has been explained in the past as a statistical phenomenon. The strength of concrete is randomly variable, and in a larger structure there is a greater chance of encountering a smaller strength, which could explain the size effect. However, since the random variations occur only within certain representative volumes of small size, the statistical size effect must lead to a horizontal asymptote. Thus, the asymptotic behavior is totally different from that we obtained for fracture mechanics. Needless to say, the fracture-type size effect appears to be the correct one.

Other Aspects

For some types of loading, especially those in dynamics, the principal tensile stress may initially cause only a partial cracking and fracture may be completed later under a principal tensile stress of a different direction. For such situations, a softening stress-strain relation that can be applied for a general loading path with rotating principal stress directions is needed. An attractive method to develop such a stress-strain relation is the microplane model [68, 69]. In this model, analogous to the well-known slip theory of plasticity [70, 71], one specifies the constitutive relation between the stresses and strains acting within the microstructure on a plane of any orientation. No tensorial invariance restrictions need to be satisfied by this relation, since they are satisfied subsequently by a suitable combination of microplanes of all possible orientations. It appeas that for the

modeling of progressive fracture, the strains from all microplanes must be constrained to the same macroscopic strain tensor, and requiring that the energy dissipation must be the same whether expressed macroscopically or microscopically, one finds that the inelastic stress relaxations from all microplanes must be superimposed, evaluating a certain integral over a unit hemisphere. This model has been shown [69] to be able to represent tensile strain softening of concrete. Furthermore, it was shown that the same model can describe the shear resistance of cracks and their dilatancy caused by shear [72].

While the microplane model represents a refinement of the crack band model, a simplified approach is also of interest. It has been recently investigated whether concrete fracture can be predicted by an approximate equivalent linearly elastic fracture analysis based on the concept of R-curves (resistance curves) known from fracture analysis of metals [73]. This approach is based on two hypotheses: 1) for the purpose of determining the energy release rate, the crack length a is not required to represent the actually measured crack length but permits a to be any fictitious crack length. 2) The fracture energy G_c is not a constant but varies as a function of the extension c of the fictitious crack from the body surface or a notch ($c = a - a_0$ where a_0 = notch length; Fig. 12). In the second hypothesis, the dependence of fracture energy on crack extension is supposed to be unique, as proposed for metals by Krafft et al. [50, 31]. This is certainly a simplification, since in reality the R-curve is different for different body geometries, different loading arrangements, different loading paths, etc., and indeed the R-curves calculated by finite elements from the blunt crack band theory as explained before exhibit such a dependence. Nevertheless,

for many situations, a unique curve of fracture energy versus crack extension, called the R-curve, is an acceptable approximation (Fig. 12).

In the R-curve approach, the critical state of failure is obtained when the following two conditions are satisfied [31]:

$$W'(a) = G_c(c), \qquad \frac{\partial W'(a)}{\partial a} = \frac{\partial G_c(c)}{\partial c} \tag{17}$$

in which $W'(a) = \partial W/\partial a$ = energy release rate of the body, and $c = a - a_0$. In elastic fracture mechanics, the energy release rate function has the form $W'(a) = P^2 W_1'(a)$, in which $W_1'(a)$ is the energy release rate function for $P = 1$. Substituting this relation into Eq. 16, one has two equations for two unknowns c and the failure load P. These two equations are nonlinear and have to be solved iteratively. However, if the function $G_c(c)$ is assumed to be a parabola and the function $W_1'(a)$ to be a straight line, then Eq. 15 can be reduced to a single quadratic equation for P [31].

The bulk of fracture test data was analyzed using the R-curve approach [73]. Various algebraic expressions have been used for the R-curve $G_c(c)$, including an exponential curve with a horizontal asymptote, a segment of a parabola terminating at its apex, after which a horizontal line follows, and a bilinear diagram. By statistical analysis of the test data available from the literature, it was found that the precise shape of the R-curve cannot be determined. The optimum fits were about equally good with the aforementioned expressions as well as other expressions. Only the initial value of G_c, the final value G_f and the overall slope, were found to be of importance. This conclusion implies that it makes no sense trying to develop sophisticated differential equations for determining the shape of the R-curves.

Therefore, the expression for the R-curve should be chosen from the viewpoint of convenience, and from this viewpoint the parabolic formula is probably best, since it yields a quadratic equation for P. Fig. 13 reproduces a plot from Ref. 73 of the theoretical versus measured values of P at failure, normalized with regard to the failure load P_0 calculated from the strength theory. The parabolic formula is used in this comparison. If the theory were perfect, the data points would have to fall on a straight line through the origin, of slope 1. The deviations from such a strain line are the measures of the error. Their coefficient of variation is only 0.06, which means that a very good approximation of the existing test results is possible.

The R-curve can be sufficiently characterized by three parameters, its initial and final values and the mean slope of the rising segment. These three material characteristics can be easiest determined by carrying out maximum load tests for three substantially different test specimens. Best probably are geometrically similar specimens of substantially different sizes. Measurements other than maximum load values are then not needed, which is a significant advantage of this approach. It is very difficult to measure other quantities such as the crack length and opening, loading and unloading compliancies at the critical state, etc., and it is attractive for practical applications to be able to avoid such measurements.

For concrete structures, it is of importance to model not only isolated fractures but also systems of cracks. Of particular interest is the system of parallel equidistant cracks which forms under a uniform tensile loading of a panel reinforced by a mesh of bars, or in a beam with longitudinal reinforcement subjected to tension or bending. For the parallel crack system,

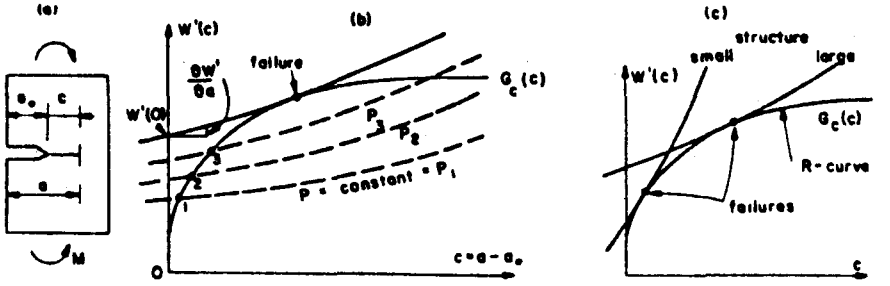

Fig. 12 - Determination of Failure with the Help of R-Curve.

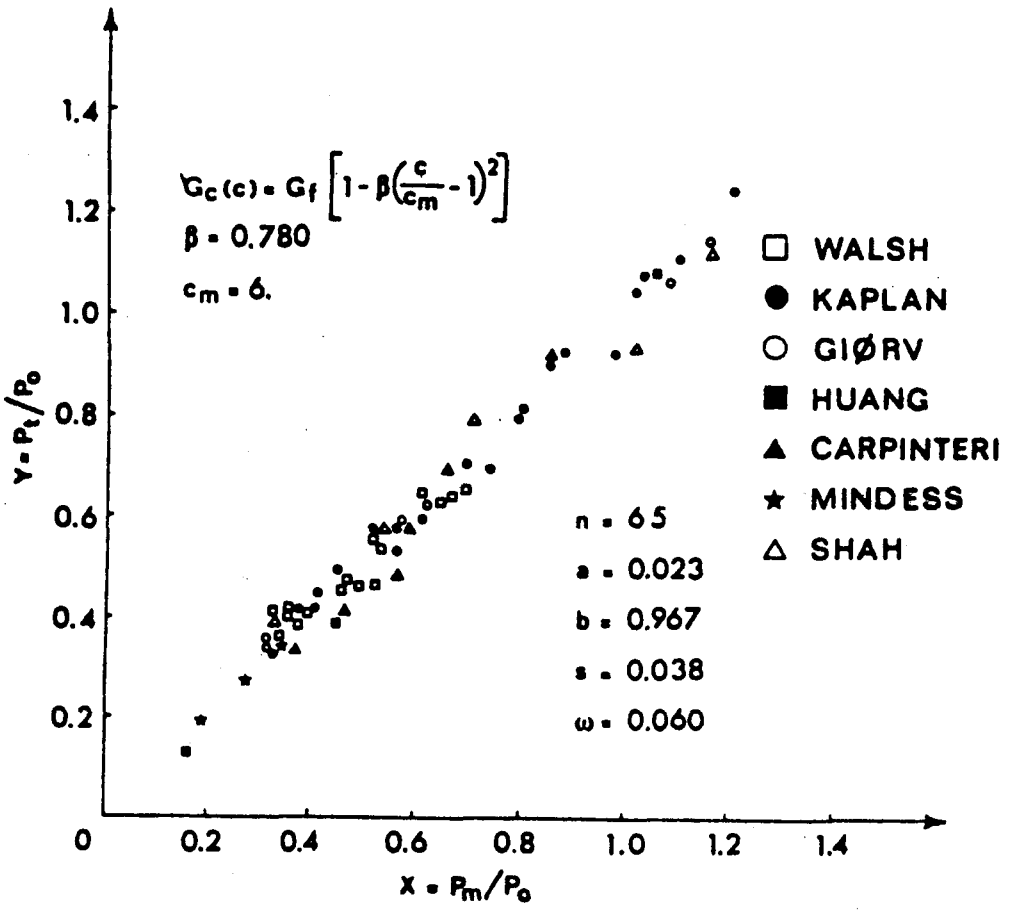

Fig. 13 - Statistical Linear Regression of Measured Failure Loads Versus Theoretical Ones.

it is necessary to determine the spacing of the cracks, after which the crack width can be estimated, and also the overall strain at which the cracks form. This problem has been traditionally analyzed on the basis of strength criteria, coupled with the conditions of bond slip. However, the strength criteria govern only the initiation of microcracking, since they pertain to the peak point of the tensile stress-strain diagram. For a complete crack formation, strain-softening must reduce the stress to zero, which means that the full strain energy under the tensile stress-strain diagram must be dissipated. Therefore, complete crack formation should properly be calculated from energy fracture criteria. This approch has been taken in Ref. 74, and simplified formulas for the crack spacing based on energy analysis were determined. Since the cracks are usually spaced rather closely compared to the maximum aggregate size, the energy balance conditions have not been written for the formation of the crack over its entire length. The formulas obtained from this fracture mechanics approach agreed reasonably well with the scant test data on crack spacing and crack width available in the literature.*

Crack width is rather important for the shear transmission capability of cracks in concrete, which is essential for the load carrying capability of concrete structures. The shear response of cracks in concrete may be characterized by an incremental relation expressing the increments of the normal and shear stress transmitted across a crack as a function relative displacement (opening) and the tangential relative displacement (slip); see Ref. 75.

*Aside from energy balance, the evolution of crack spacing of a growing crack system is also governed by certain stability conditions; see Ref. 76.

Conclusions

After a period of doubts regarding the applicability of fracture mechanics to concrete, it has now become clearly established that fracture mechanics does apply. However, a nonlinear form of fracture mechanics which takes into account the existance of a large fracture process zone ahead of the fracture front must be used. An attractive formulation is the crack band model, which is particularly suited for finite element analysis. Nevertheless, many questions remain open and much further research is needed.

Acknowledgment

Partial financial support from the U. S. National Science Foundation under grant CEE-8303148 is gratefully acknowledged. Mary Hill deserves thanks for her very prompt and careful typing of the manuscript.

References

1. Wittmann, F. H., (Editor), Fracture Mechanics of Concrete, Elsivier, Netherlands, 1983.

2. Mindess, S., "The Application of Fracture Mechanics to Cement and Concrete: A Historical Review," Chapter in State-of-the-Art Report of RILEM Technical Committee 50-FMC on "Fracture Mechanics of Concrete," ed. by F. H. Wittmann, Elsevier, Netherlands, 1983.

3. Ingraffea, A., chapter in "Fracture Mechanics Applied to Concrete Structures," ed. by G. C. Sih, Martinus Nijhoff Publishers, B.V., The Hague, Netherlands - in press.

4. Shah, S. P., chapter in "Fracture Mechanics Applied to Concrete Structures," ed. by G. C. Sih, Martinus Nijhoff Publishers, B.V., The Hague, Netherlands, - in press.

5. ASCE State-of-the-Art Report on "Finite Element Analysis of Reinforced Concrete," prepared by a Task Committee chaired by A. Nilson, Am. Soc. of Civil Engrs., New York, 1982.

6. Bazant, Z. P., "Mechanics of Fracture and Progressive Cracking in Concrete Structures," chapter in "Fracture Mechanics Applied to Concrete Structures," ed. by G. C. Sih, Martinus Nijhoff Publishers B.V., The Hague, Netherlands, - in press.

7. Rashid, Y. R., "Analysis of Prestressed Concrete Pressure Vessels," Nuclear Engng. and Design, Vol. 7, No. 4, April 1968, pp. 334-344.

8. Bazant, Z. P., "Instability, Ductility and Size Effect in Strain-Softening Concrete," J. of the Engineering Mechanics Division ASCE, Vol. 102, Apr. 1976, No. EM2, pp. 331-344 - Paper 12042.

9. Bazant, Z. P., and Panula, L., "Statistical Stability Effects in Concrete Failure," J. of the Engineering Mechanics Division, ASCE, Vol. 104. Oct. 1978, No. EM5, pp. 1195-1212, Paper 14074.

10. Bazant, Z. P., "Crack Band Model for Fracture of Geomaterials," Proc., 4th Intern. Conf. on Numerical Methods in Geomechanics, held in Edmonton, Alberta, Canada, June 1982, ed. by Z. Eisenstein, Vol. 3.

11. Bazant, Z. P., and Oh, B. H., "Crack Band Theory for Fracture of Concrete," Materials and Structures (RILEM, Paris), Vol. 16, 1983, in press (based on Ref. 130).

12. Bazant, Z. P., and Cedolin, L., "Blunt Crack Band Propagation in Finite Element Analysis," Journal of the Engineering Mechanics Division, ASCE, Vol. 105, No. EM2, Proc. Paper 14529, April 1979, pp. 297-315.

13. Bazant, Z. P., and Cedolin, L., "Fracture Mechanics of Reinforced Concrete," Journal of the Engineering Mechanics Division, ASCE, Vol. 106, No. EM6, Proc. Paper 15917, December 1980, pp. 1287-1306; with Discussion and Closure in Vol. 108, 1982, EM., pp. 464-471.

14. Cedolin, L., and Bazant, Z. P., "Effect of Finite Element Choice in Blunt Crack Band Analysis," Computer Methods in Applied Mechanics and Engineering, Vol. 24, No. 3, December 1980, pp. 305-316.

15. Bazant, Z. P., and Cedolin, L., "Finite Element Modeling of Crack Band Propagation," Journal of Structural Engineering, ASCE, Vol. 109, No. ST2, Feb. 1983, pp. 69-92.

16. Bazant, Z. P., Pfeiffer, P., Marchertas, A. H., "Blunt Crack Band Propagation in Finite Element Analysis for Concrete Structures," Preprints 7th Int. Conf. on Structural Mechanics in Reactor Technology, Chicago, Aug. 1983.

17. Bazant, Z. P., and Oh, B. H., "Rock Fracture via Stress-Strain Relations," Concrete and Geomaterials, Report No. 82-11/665r, Northwestern University, Evanston, Illinois, Nov. 1982.

18. Mindess, S., and Diamond, S., "A Preliminary SEM Study of Crack Propagation in Mortar," Cement and Concrete Research, Vol. 10, 1980, pp. 509-519.

19. Cedolin, L., Dei Poli, S., and Iori, L., "Experimental Determination of the Fracture Process Zone in Concrete," Cement and Concrete Research, Vol. 13, 1983 - to appear.

20. Cedolin, L., Dei Poli, S., and Iori, L., "Experimental Determination of the Stress-Strain Curve and Fracture Zone for Concrete in Tension," Proc., Int. Conf. on Constitutive Laws for Engineering Materials, ed. by C. Desai, University of Arizona, Tucson, January 1983.

21. Barenblatt, G. I., "The Formation of Equilibrium Cracks During Brittle Fracture, General Ideas and Hypothesis. Axially-Symmetric Cracks," Prikladnaya Matematika i Mekhanika, Vol. 23, No. 3, 1959, pp. 434-444.

22. Dugdale, D. S., "Yielding of Steel Sheets Containing Slits," J. Mech. Phys. Solids, Vol. 8, 1960, pp. 100-108.

23. Kfouri, A.P., and Miller, .K. J., "Stress Displacement, Line Integral and Closure Energy Determinations of Crack Tip Stress Intensity Factors," Int. Journal of Pres. Ves. and Piping, Vol. 2, No. 3, July 1974, pp. 179-191.

24. Kfouri, A. P., and Rice, J. R., "Elastic/Plastic Separation Energy Rate for Crack Advance in Finite Growth Steps," in "Fracture 1977" (Proc. of the 4th Intern. Conf. on Fracture, held in Waterloo, Ontario, June 1977), ed. by D. M. R. Taplin, University of Waterloo Press 1977, Vol. 1, pp. 43-59.

25. Knauss, W. C., "On the Steady Propagation of a Crack in a Viscoelastic Sheet; Experiments and Analysis," in The Deformation in Fracture of High Polymers, ed. by H. H. Kausch, Pub. Plenum Press, 1974, pp. 501-541.

26. Wnuk, M. P., "Quasi-Static Extension of a Tensile Crack Contained in Viscoelastic Plastic Solid," Journal of Applied Mechanics, ASME, Vol. 41, 1974, No. 1, pp. 234-248.

27. Hillerborg, A., Modéer, M., and Petersson, P. E., "Analysis of Crack Formation and Crack Growth in Concrete by Means of Fracture Mechanics and Finite Elements," Cement and Concrete Research, Vol. 6, 1976, pp. 773-782.

28. Petersson, P. E., "Fracture Energy of Concrete: Method of Determination," Cement and Concrete Research, Vol. 10, 1980, pp. 78-89, and "Fracture Energy of Concrete: Practical Performance and Experimental Results," Cement and Concrete Research, Vol. 10, 1980, pp. 91-101.

29. Knott, J. F., "Fundamentals of Fracture Mechanics," Butterworths, London, England, 1973.

30. Parker, A. P., "The Mechanics of Fracture and Fatigue, E. & F. N. Spon, Ltd. - Methuen, London, 1981.

31. Broek, D., "Elementary Engineering Fracture Mechanics," Noordhoff International Publishing, Leyden, Netherlands, 1974.

32. Evans, R. H., and Marathe, M. S., "Microcracking and Stress-Strain Curves for Concrete in Tension," Materials and Structures (RILEM, Paris), No. 1, Jan.-Feb., 1968, pp. 61-64.

33. Brown, J. H., "Measuring the Fracture Toughness of Cement Paste and Mortar," Magazine of Concrete Research, Vol. 24, No. 81, December 1972, pp. 185-196.

34. Carpinteri, A., "Experimental Determination of Fracture Toughness Parameters K_{IC} and J_{IC} for Aggregative Materials," Advances in Fracture Research," (Proc., 5th International Conference on Fracture, Cannes, France, 1981) ed. by D. Francois, Vol. 4, pp. 1491-1498.

35. Carpinteri, A., "Static and Energetic Fracture Parameters for Rocks and Concretes," Report, Instituto di Scienza delle Costruzioni-Ingegneria, University of Bologna, Italy, 1980.

36. Entov, V. M., and Yagust, V. I., "Experimental Investigation of Laws Governing Quasi-Static Development of Macrocracks in Concrete,: Mechanics of Solids (translation from Russian), Vol. 10, No. 4, 1975, pp. 87-95.

37. Gjørv, O. E., Sørensen, S. I., and Arnesen, A., "Notch Sensitivity and Fracture Toughness of Concrete," Cement and Concrete Research, Vol. 7, 1977, pp. 333-344.

38. Huang, C. M. J., "Finite Element and Experimental Studies of Stress Intensity Factors for Concrete Beams," Thesis Submitted in Partial Fulfillment of the Requirements for the Degree of Doctor of Philosophy, Kansas State University, Kansas, 1981.

39. Kaplan, M. F., "Crack Propagation and the Fracture of Concrete," American Concrete Institute Journal, Vol. 58, No. 11, November 1961.

40. Kesler, C. E., Naus, D. J., and Lott, J. L., "Fracture Mechanics - Its Applicability to Concrete," International Conference on the Mechanical Behavior of Materials, Kyoto, August 1971.

41. Mindes, S., Lawrence, F. V., and Kesler, C. E., "The J-Integral As a Fracture Criterion for Fiber Reinforced Concrete," Cement and Concrete Research, Vol. 7, 1977, pp. 731-742.

42. Naus, D. J., "Applicability of Linear-Elastic Fracture Mechanics to Portland Cement Concretes," Thesis Submitted in Partial Fulfillment of the Requirements for the Degree of Doctor of Philosophy, University of Illinois at Urbana-Champaign, 1971.

43. Shah, S. P., and McGarry, F. J., "Griffith Fracture Criterion and Concrete," Journal of the Engineering Mechanics Division, ASCE, Vol. 97, No. EM6, Proc. Paper 8597, December 1971, pp. 1663-1676.

44. Shah, S. P., chapter in "Fracture Mechanics Applied to Concrete Structures," ed. by G. C. Sih, Martinus Nijhoff Publishers, B.V., The Hague, Netherlands, - in press.

45. Sok, C., Baron, J., and Francois, D., "Mécanique de la Rupture Appliquée au Beton Hydraulique," Cement and Concrete Research, Vol. 9.

46. Swartz, S. E., Hu, K. K., Fartash, M., and Huang, C. M. J., "Stress Intensity Factors for Plain Concrete in Bending - Prenotched Versus Precracked Beams," Report, Department of Civil Engineering, Kansas State University, Kansas, 1981.

47. Walsh, P. F., "Fracture of Plain Concrete,: The Indian Concrete Journal, Vol. 46, No. 11, November 1979, pp. 469, 470, and 476.

48. Wecharatana, M., and Shah, S. P., "Resistance to Crack Growth in Portland Cement Composites," Report, Department of Material Engineering, University of Illinois at Chicago, Chicago, Illinois, Nov. 1980.

49. Petersson, P. C., "Crack Growth and Development of Fracture Zones in Plain Concrete and Similar Materials," Doctoral Dissertation, Lund Institute of Technology, Lund, Sweden, Dec. 1981.

50. Krafft, J. M., Sullivan, A. M., Boyle, R. W., "Effect of Dimensions on Fast Fracture Instability of Notched Sheets," Cranfield Symposium, 1961, Vol. I, pp. 8-28.

51. Evans, R. H., and Marathe, M. S., "Microcracking and Stress-Strain Curves for Concrete in Tension," Materials and Structures (RILEM, Paris), No. 1, Jan.-Feb., 1968, 61-64.

52. Heilmann, H. G., Hilsdorf, H. H., and Finsterwalder, K., "Festigkeit und Verformung von Beton unter Zugspanungen," Deutscher Ausschuss für Stahlbeton, Heft 203, W. Ernst & Sohn, West Berlin, 1969.

53. Rüsh, H., and Hilsdorf, H., "Deformation Characteristics of Concrete Under Axial Tension," Voruntersuchungen, Bericht Nr. 44, Munich, May 1963.

54. Pan, Y. C., Marchertas, A. H., and Kennedy, J. M., "Finite Element of Blunt Crack Band Propagation," A Modified J-Integral Approach, Preprints 7th Intern. Conf. on Structural Mechanics in Reactor Technology, Paper H, Chicago, Aug. 1983.

55. Marchertas, A. H., Kulak, R. F., and Pan. Y. C., "Performance of Blunt Crack Approach Within a General Purpose Code," in Nonlinear Numerical Analysis of Reinforced Concrete, ed. by L. E. Schwer, Am. Soc. of Mech. Engrs., New York 1982, (presented at ASME Winter Annual Meeting, Phoenix, Nov. 1982), pp. 107-123.

56. Pan, Y. C., and Marchertas, A. H., Private Communication, May 1983, at Argonne National Laboratory, Argonne, IL.

57. Bažant, Z. P., and Pfeiffer, P., "Finite Element Crack Band Analysis," in preparation.

58. Bažant, Z. P., Pfeiffer, P., and Marchertas, A. H., "Blunt Crack Band Propagation in Finite Element Analysis for Concrete Structures," Preprints 7th Int. Conf. on Structural Mechanics in Reactor Technology, Chicago, Aug. 1983.

59. Bažant, Z. P., "Size Effect in Brittle Failure of Concrete Structures," Report No. 83-2/665s, Center for Concrete and Geomaterials, Northwestern University, Evanston, Illinois, Feb. 1983.

60. Bažant, Z. P., and Kim. J. K., "Size Effect in Shear Failure of Reinforced Concrete Beams," Report No. 83-5/428s, Center for Concrete and Geomaterials, Northwestern University, Evanston, Illinois, May 1983.

61. Kani, G. N. J., "Basic Facts Concerning Shear Failure," Part I and Part II, J. of ACI, Vol. 63, No. 6, June 1966, pp. 675-692.

62. Leonhardt, F., and Walther, R., "Beiträge zur Behandlung der Schubprobleme im Stahlbetonbau," Beton-u Stahlbetonbau, Vol. 56, No. 12 (1961), Vol. 57 No. 2, 3, 6, 7, 8, (1962), Vol. 58, No. 8, 9 (1963).

63. Bhal, N. S., "Über den Einfluss der Balkenhöhe auf Schubtragfähihkeit von einfeldrigen Stahlbetonbalken mit und ohne Schubbewehrung, Dissertation, Universität Stuttgärt, 1968.

64. Walraven, J. C., "The Influence of Depth on the Shear Strength of Lightweight Concrete Beams without Shear Reinforcement," Stevin Laboratory Report No. 5-78-4, Delft University of Technology 1978.

65. Taylor, H. P. J., "The Shear Strength of Large Beams," J. of the Structural Division ASCE, Vol. 98, 1972, pp. 2473-2490.

66. Rüsch, M., Haugli, F. R., and Mayer, M., "Schubversuche an Stahlbeton Rechteckbalken mit Gleichmässig Verteilter Belastung," Deutscher Ausschuss für Stahlbeton, Heft 145, W. Ernst u. Sohn, West Berlin 1962.

67. Swamy, R. N., and Qureshi, S. A., "Strength, Cracking and Deformation Similitude in Reinforced T-Beams under Bending and Shear," Part I and II, J. of Am. Concrete Inst., Vol. 68, No. 3, 1971, pp. 187-195.

68. Bazant, Z.P., and Oh, B. H., "Microplane Model for Fracture Analysis of Concrete Structures," Proc. Symp. on the "Interaction of Nonnuclear Munitions with Structures," U. S. Air Force Academy, Colorado Springs, May 1983, pp. 49-55.

69. Bazant, Z. P., and Oh, B. H., "Model of Weak Planes for Progressive Fracture of Concrete and Rock," Report No. 83-2/448m, Center for Concrete and Geomaterials, Northwestern University, Evanston, Il., Feb. 1983.

70. Taylor, G. I., "Plastic Strain in Metals," J. Inst. Metals, Vol. 63, 1938, pp. 307-324.

71. Batdorf, S. B., and Budiansky, B., "A Mathematical Theory of Plasticity Based on the Concept of Slip," NACA TN 1871, April, 1949.

72. Bazant, Z. P., and Gambarova, P., "Crack Shear in Concrete: Crack Band Microplane Model", in preparation.

73. Bazant, Z. P., and Cedolin, L., "Approximate Linear Analysis of Concrete Fracture by R-Curves," Report No. 83-7/679a, Center for Concrete and Geomaterials, Technological Institute, Northwestern University, Evanston, Illinois, July 1983.

74. Bazant, Z. P., and Oh, B. H., "Spacing of Cracks in Reinforced Concrete," J. of Engng. Mech. ASCE.

75. Bazant, Z. P., and Gambarova, P., "Rough Cracks in Reinforced Concrete," J. of the Struct. Div., Proc. ASCE, Vol. 106, 1980, pp. 819-842; Disc. pp. 2579-2581.

76. Bazant, Z. P., Ohtsubo, H., Aoh, K., "Stability and Post-Critical Growth of a System of Cooling or Shrinkage Cracks," International Journal of Fracture, Vol. 15, No. 5., Oct. 1979, pp. 443-456.